

Comparative Impact Analysis of Tap Winding Order and Configuration on Transformer Short-Circuit Inductance

Mahsa Taghilou*, Mojtaba Mirsalim**(C.A.)

Abstract: In contemporary power systems, it is crucial to ensure stable voltage levels to mitigate the fluctuations resulting from diverse load conditions. On-load tap changers (OLTCs) play a pivotal role in addressing these fluctuations by dynamically adjusting the number of turns in the transformer winding. This study investigates the integration of OLTCs within transformer designs, focusing on various methodologies related to tap winding order and configurations, which are vital for both electrical and magnetic performance. A comprehensive review of the operational principles governing different types of OLTCs is provided, highlighting their significance in voltage regulation. Furthermore, this paper analyzes the impact of linear OLTC winding order on the short-circuit impedance of a 30 MVA transformer. The findings underscore the importance of OLTC selection and design in optimizing transformer performance.

Keywords: on-load tap changers, short-circuit impedance, winding order and configuration

1 Introduction

As the power network continues to expand, the necessity for effective voltage regulation has become increasingly critical. Tap changers, integral components of transformers, play a pivotal role in maintaining voltage stability across varying load conditions [1],[2]. By adjusting the turn ratio, these devices actively mitigate voltage fluctuations, thereby enhancing the reliability and efficiency of power delivery systems [3]. Tap changers are utilized in two types: on-load tap changers (OLTCs) and de-energized tap changers (DETCs). DETCs are commonly employed to manually adjust the voltage levels between two interconnected systems which facilitate the alignment of voltage parameters before system integration. In contrast, OLTCs operate automatically within a system, dynamically responding to daily fluctuations in voltage levels and enabling high-frequency adjustments that enhance system stability and performance. On-Load Tap Changers (OLTCs) are categorized based on their application to the

transformer windings into three primary types which are linear, reverse, and coarse-fine [4],[5]. As illustrated in Fig. 1, these three categories are exemplified using a transformer equipped with a 19-step tap changer. In the linear configuration, all 19 steps are positioned on a single winding, resulting in a high-voltage output that increases proportionally with the steps from 1 to 19. In this scenario, the nominal step is defined as step 10. Conversely, in the reverse configuration, 9 steps are placed on the tap changer winding. Depending on the orientation of the winding with the high voltage side, either direct or reverse, as determined by a switch, the voltage level can either increase or decrease. The coarse-fine design incorporates both fine and coarse windings. Initially, 9 steps from the fine winding are introduced into the circuit. At the nominal tap position, the coarse winding is simultaneously engaged with the HV winding. If further voltage elevation is required, the fine winding can be reintroduced into the circuit.

Iranian Journal of Electrical & Electronic Engineering, YYYY.
Paper first received DD MONTH YYYY and accepted DD MONTH YYYY.

* Department of Electrical Engineering,
Amirkabir University of Technology, Tehran, Iran.
E-mail: m.taghilou@aut.ac.ir

** Department of Electrical Engineering,
Amirkabir University of Technology, Tehran, Iran.
E-mails:
mirsalim@aut.ac.ir, mojtaba_mirsalim@yahoo.com
Corresponding Author: Mojtaba Mirsalim

Power transformers are typically designed for a service life of 20–25 years (approximately 7500 days). Throughout this period, however, they may be subjected to fault conditions that result in short circuits, producing currents far exceeding their rated operating levels. Such elevated currents can impose substantial electromechanical stresses on the transformer windings, potentially leading to severe mechanical deformation or failure [6]. The magnitude of short-circuit current is directly influenced by the transformer's short-circuit impedance, which is itself dependent on the design and implementation of the windings. In addition, the distribution of the magnetic field, determined by both the winding configuration and the relative order of the windings, affects the stored magnetic energy and consequently the short-circuit impedance. Therefore, the selection of the tap-changer configuration and the arrangement of the associated windings constitute critical design factors that significantly affect a transformer's short-circuit impedance and its ability to withstand fault conditions [7]. Deviations from the standard impedance can significantly affect both the design cost and the physical footprint of transformers. According to IEEE C57.12.00 standards, a tolerance of $\pm 7.5\%$ is permitted for two-winding transformers, while a tolerance of $\pm 10\%$ is allowed for three-winding transformers regarding short-circuit impedance [8],[9]. As the electrical resistance component of short-circuit impedance is relatively insignificant [10], this paper aims to assess the variations in short-circuit impedance resulting from changes in leakage inductance across different tap winding order and configuration. To calculate the short-circuit inductance of a transformer, two general methods can be employed which are analytical and numerical approaches. The analytical method allows for a reasonably accurate overview of the transformer's inductance by simplifying assumptions [11]–[14]. Conversely, the numerical method yields more precise results by addressing the actual conditions of the problem [15],[16]. In this paper, the analytical approach will be utilized to examine the differences in short-circuit inductance of a transformer based on various methods of applying the tap changer windings of the transformer.

2 Short-Circuit Impedance

In electrical installations, accurate calculation of short-circuit currents at various network points is essential for proper sizing of equipment and ensuring the protection of life and property which is critical for the design and safety of electrical systems. A short-circuit refers to an electrical connection between phases or to ground, with significant implications for transformer design, particularly concerning single line-to-ground faults and three-phase symmetrical faults (phase-to-ground: 80% of faults, phase-to-phase: 15% of faults, and three-phase: only 5% of initial faults). Such faults result in excessive current

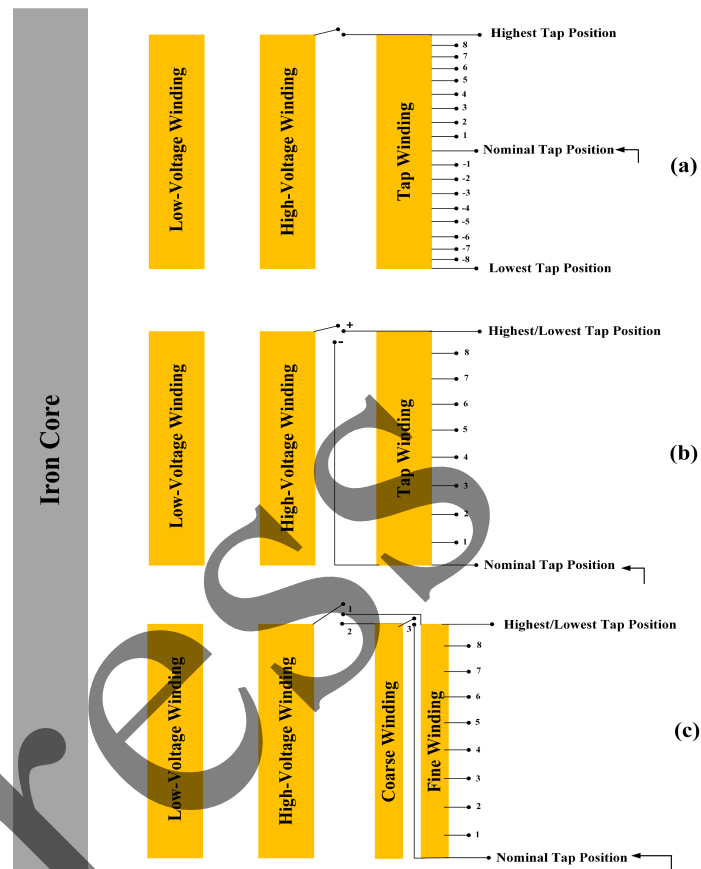


Fig.1 Three primary types of on-load tap changer
(a) linear, (b) reverse, (c) coarse-fine

flowing through the circuit, leading to consequences that range from minor malfunctions to catastrophic failures. The severity of these consequences depends on the impedance, Z_{SC} to handle current, I_{SC} during short-circuit conditions and the duration for which the current is allowed to flow without causing damage to the connected equipment [17].

As the number of taps in a tap changer is altered, the electrical characteristics of the windings, including resistance and reactance, are also affected. Consequently, the short-circuit impedance of the transformer will change

accordingly. To maintain compliance with standard requirements regarding the percentage impedance range, as well as to account for the variations in the configurations of different types of tap changers that lead to differences in the electrical characteristics of transformers, it is essential to conduct a thorough analysis of these differences for optimal and accurate design.

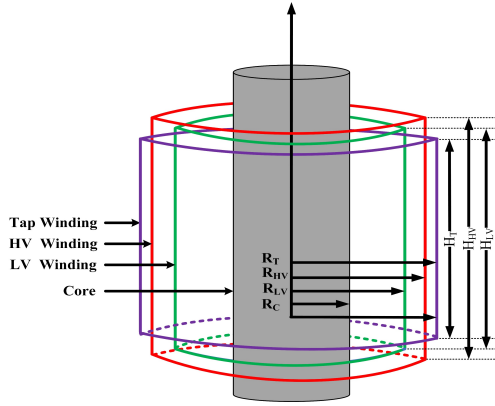


Fig.2 Single-leg model of the proposed transformer

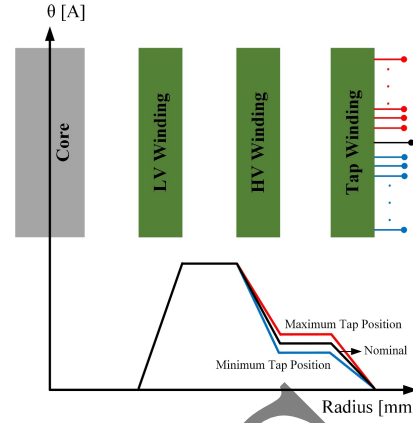


Fig.3 2D geometric model of MMF distribution of linear OLTC

3 Analytical Method for Calculating Inductance

The analytical method presented provides a robust framework for calculating the inductance of transformers. This method typically relies on established formulas and assumptions about the transformer's physical characteristics. The analytical approach also assumes ideal conditions, such as uniform magnetic fields and perfect coupling between windings. Fig.2 illustrates a single-leg model of the proposed transformer including the core and the windings. The windings are arranged concentrically in a cylindrical form on the core leg, designated as low voltage (LV) winding, high voltage (HV) winding, and tap winding with respective heights of H_{LV} , H_{HV} , and H_T . The radius from the center of the core to each winding is denoted as R_{LV} , R_{HV} , and R_T . As observed in Fig. 1 and Fig. 2, the structures of the linear and reverse types of tap windings are similar. In the coarse-fine type, the tap changer consists of two windings, resulting in four windings per phase. The analytical method for calculating the short-circuit inductance of the transformer equipped with each type of tap changer will be examined further.

3.1 Linear Tap Changer

The linear tap changer consists of an auxiliary winding connected in series with the high-voltage (HV) winding, enabling continuous tap adjustments to achieve the specified range of maximum and minimum voltage regulation. In this configuration, the nominal tap corresponds to the central position. By raising or lowering the tap position along the tap winding, all designated voltage levels of the transformer can be obtained. The ampere-turn distribution is evaluated by considering the geometric parameters of the transformer, as illustrated in Fig. 3 and expressed in Equations (1) and (2) [14]. The parameters R_1 through R_6 represent the inner and outer radii of the LV, HV, and tap windings, respectively, as listed in Table 1. The ampere-turn distribution is described in Eq. (1), where θ , B , μ_0 , and H_{eq} denote the

angular position, magnetic flux density, permeability of free space, and equivalent winding height, respectively. Additionally, B_w denotes the radial depth of the windings.

$$B(r) = \mu_0 \frac{\theta(r)}{H_{eq}} = \frac{\mu_0}{H_{eq}} \begin{cases} \frac{(r - R_1)}{(R_2 - R_1)} \theta_1, & R_1 < r < R_2 \\ \theta_1, & R_2 < r < R_3 \\ \frac{(r - R_3)}{(R_4 - R_3)} (\theta_2 - \theta_1) + \theta_1, & R_3 < r < R_4 \\ \theta_2, & R_4 < r < R_5 \\ \frac{(R_6 - r)}{(R_6 - R_5)} \theta_2, & R_5 < r < R_6 \end{cases} \quad (1)$$

$$\begin{aligned} R_1 &= R_{LV} & R_2 - R_1 &= B_{w1} \\ R_3 &= R_{HV} & R_4 - R_3 &= B_{w2} \\ R_5 &= R_{Tap} & R_6 - R_5 &= B_{w3} \end{aligned} \quad (2)$$

Table 1. Geometrical parameters of the proposed transformer.

Windings	Inner Radius [mm]	Outer Radius [mm]	Height [mm]
LV	320	388	966
HV	412	486.5	914
Coarse	511.5	522	720
Fine	537	549	630
Tap	511.5	522	630

Table 2. Electrical parameters of the proposed transformer.

Parameter	Value	Unit
Rated Power	30	MVA
Rated High Voltage	63	kV
Rated Low Voltage	20	kV
Rated HV-side Current	275	A
Rated LV-side Current	866	A
HV-Winding Turn	355	turn
LV-Winding Turn	234	turn
Voltage Regulation	63±15%	kV
Tapping Range	±9×1.67%	kV
HV Winding Connection	Star	Y
LV Winding Connection	Delta	Δ
Short-Circuit Impedance	10	%
Frequency of Grid	50	Hz

3.2 Reverse Tap Winding

The reverse tap changer consists of a series-connected winding and a switching mechanism capable of operating in two modes: direct connection and reverse connection to the HV winding. Tap adjustments are performed to obtain the required maximum and minimum voltage levels. As illustrated in Fig. 4, the nominal tap in this configuration corresponds to the center tap, considering the dual-function operation of the switch. By varying the tap position along the winding, all designated voltage levels of the transformer can be achieved.

The magnetic flux density during reverse-switch operation is characterized by Equations (3) and (4). These expressions describe the distribution of the magnetic field under reverse tap-changing conditions. [16]:

$$B(r) = \mu_0 \frac{\theta(r)}{H_{eq}} = \frac{\mu_0}{H_{eq}} \begin{cases} \frac{(r-R_1)}{(R_2-R_1)}\theta_1, R_1 < r < R_2 \\ \theta_1, R_2 < r < R_3 \\ \frac{(R_3-r)}{(R_4-R_3)}(\theta_2 + \theta_1) + \theta_1, R_3 < r < R_4 \\ -\theta_2, R_4 < r < R_5 \\ \frac{(r-R_6)}{(R_6-R_5)}\theta_2, R_5 < r < R_6 \end{cases} \quad (3)$$

$$\begin{aligned} R_1 &= R_{LV} & R_2 - R_1 &= B_{w1} \\ R_3 &= R_{HV} & R_4 - R_3 &= B_{w2} \\ R_5 &= R_{Tap} & R_6 - R_5 &= B_{w3} \end{aligned} \quad (4)$$

All parameters related to Eq.3 and Eq.4 are similar to the parameters of the linear tap changer. Additionally, the magnetic field density, under direct operation of the switch, is similar to the magnetic field density of linear tap changer.

3.3 Coarse-Fine Tap Winding

The coarse-fine tap changer comprises two series-connected windings and an associated switching mechanism linked to the HV winding, enabling all tap adjustments necessary to achieve the specified maximum and minimum voltage levels. In this configuration, the nominal tap is defined as the zero tap, based on the series connection of the coarse winding with the HV winding.

The operation of the coarse-fine tap changer occurs in three sequential stages, progressing from the lower tap position to the upper tap. Initially, the fine winding is connected in series with the HV winding, increasing the output voltage from the minimum level up to the nominal value of the transformer. At this stage, the coarse winding remains disconnected once the nominal voltage is obtained through the HV winding alone. If a voltage level above the nominal value is required, the fine winding is reintroduced into the circuit and connected in series with both the coarse and the HV windings. The magnetic flux density corresponding to each operational stage is expressed in Equations (5) and (6). Considering the

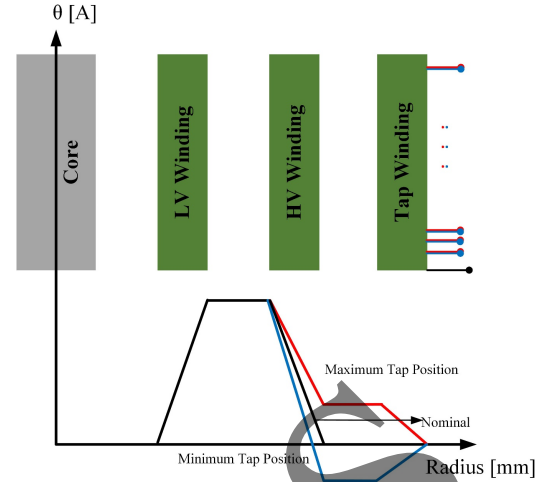


Fig.4 2D geometric model of MMF distribution of reverse OLTC

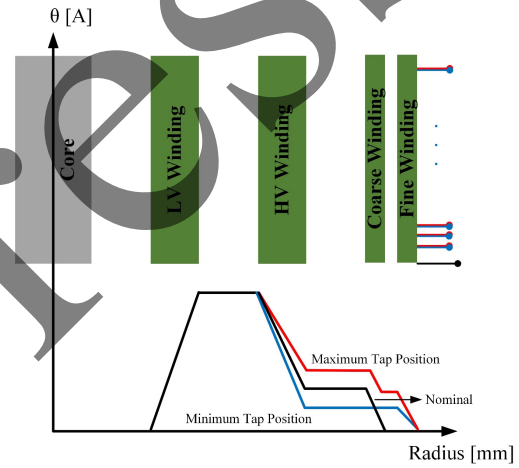


Fig.5 2D geometric model of MMF distribution of coarse-fine OLTC

analytical method used for evaluating transformer inductance, based on the axial distribution of magnetic flux, and incorporating the fringing effects at the upper and lower boundaries of the windings, the Rogowski factor is applied for determining the effective winding height, as described in Equations (7) to (9).

Tables 3, 4, and 5 present the ampere-turn values for each operating step of the Linear, Reverse, and Coarse-Fine tap changers, respectively. These values are derived from the parameters listed in Table 2 and are expressed in per-unit on the low-voltage side.

Finally, by employing the magnetic field distributions obtained from the aforementioned analytical relations and applying the magnetic-energy method, the short-circuit Inductance of the transformer are calculated in accordance with Equations (10) to (13).

$$B(r) = \mu_0 \frac{\theta(r)}{H_{eq}} = \frac{\mu_0}{H_{eq}} \begin{cases} \frac{(r-R_1)}{(R_2-R_1)} \theta_1, R_1 < r < R_2 \\ \theta_1, R_2 < r < R_3 \\ \frac{(r-R_3)}{(R_4-R_3)} (\theta_2 - \theta_1) + \theta_1, R_3 < r < R_4 \\ \theta_2, R_4 < r < R_5 \\ \frac{(r-R_5)}{(R_6-R_5)} (\theta_3 - \theta_2) + \theta_2, R_5 < r < R_6 \\ \theta_3, R_6 < r < R_7 \\ \frac{(R_8-r)}{(R_8-R_7)} \theta_3, R_7 < r < R_8 \end{cases} \quad (5)$$

$$\begin{aligned} R_2 &= R_{LV} & R_2 - R_1 &= B_{w_1} \\ R_4 &= R_{HV} & R_4 - R_3 &= B_{w_2} \\ R_6 &= R_{Coarse} & R_6 - R_5 &= B_{w_3} \\ R_8 &= R_{Fine} & R_8 - R_7 &= B_{w_4} \end{aligned} \quad (6)$$

$$H_{eq} = \frac{H_w}{K_{Rog}} \quad (7)$$

$$K_{Rog} = 1 - \frac{1 - e^{\frac{-\pi H_w}{\sum_{i=1}^n B_{w_i}}}}{\frac{\pi H_w}{\sum_{i=1}^n B_{w_i}}} \quad (8)$$

$$H_w = \sum_{i=1}^n \frac{\theta_i H_i}{\theta_i} \quad (9)$$

$$\frac{1}{2} L_{Short-Circuit} I_1^2 = \frac{1}{2\mu_0} \int B^2 dv \quad (10)$$

$$U_k \% = \frac{X_{Short-Circuit}}{Z_b} \times 100 \quad (11)$$

$$X_{Short-Circuit} = \omega L_{Short-Circuit} \quad (12)$$

$$Z_b = \frac{V_b}{I_b} \quad (13)$$

4 Winding Order

In transformers, impedance is not a fixed parameter; rather, it varies depending on the load conditions. The term impedance swing refers to the variations in impedance that occur as the load fluctuates. These changes in load can cause significant fluctuations in transformer performance, resulting in corresponding changes in impedance. Maintaining a stable impedance profile, where impedance remains relatively constant despite load variations, is critical to minimizing voltage fluctuations and other performance issues.

Transformer stability is essential to ensure efficient and reliable operation, reducing losses and preventing overheating. Understanding the relationship between winding configuration and impedance swings is therefore crucial for designing transformers capable of handling dynamic electrical demands without compromising efficiency or operational stability. This consideration is especially important in applications subjected to frequent

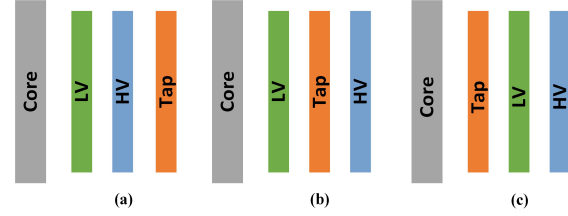


Fig.6 Winding order

load changes, such as power distribution networks and renewable energy systems. Impedance swings at taps with high impedance can cause pronounced voltage drops on the secondary side during transformer loading. When the transformer operates at these high-impedance taps, the interaction between increased load current and elevated impedance results in greater voltage drops across the windings, leading to reduced secondary voltage output. Conversely, a substantial reduction in short-circuit impedance may increase short-circuit forces within the transformer, exerting additional stress on insulation materials. This can accelerate insulation breakdowns and increase the likelihood of short circuits, thereby undermining transformer reliability due to mechanical and thermal stresses.

To mitigate such risks, adjusting the winding order during the design phase is essential to control and minimize excessive impedance swings. Furthermore, these impedance variations also affect transformer core losses, including hysteresis and eddy current losses. Although copper losses primarily depend on winding resistance, changes in current caused by varying inductance indirectly influence these losses as well. Therefore, both incremental and decremental variations in inductance during tap operations significantly impact transformer performance. Given that altering the relative positioning of windings affects the ampere-turn distribution, and consequently modifies the short-circuit impedance, this study investigates the impact of winding position changes in the case of a linear OLTC.

As shown in Fig. 6, the ampere-turn distribution in all three scenarios follows a relation similar to Eq. (1), with the primary variation arising from changes in radial distance parameters, as described in Eq. (14).

$$\begin{aligned} R_1 &= R_{LV} & R_2 - R_1 &= B_{w_1} \\ R_3 &= R_{HV} & R_4 - R_3 &= B_{w_2} \\ R_5 &= R_{Tap} & R_6 - R_5 &= B_{w_3} \end{aligned} \quad (14-a)$$

$$\begin{aligned} R_1 &= R_{LV} & R_2 - R_1 &= B_{w_1} \\ R_3 &= R_{Tap} & R_4 - R_3 &= B_{w_2} \\ R_5 &= R_{HV} & R_6 - R_5 &= B_{w_3} \end{aligned} \quad (14-b)$$

$$\begin{aligned} R_1 &= R_{Tap} & R_2 - R_1 &= B_{w_1} \\ R_3 &= R_{LV} & R_4 - R_3 &= B_{w_2} \\ R_5 &= R_{HV} & R_6 - R_5 &= B_{w_3} \end{aligned} \quad (14-c)$$

Considering the change in the arrangement of the windings relative to each other, Tables 3 to 5 show the radial distances of each winding in each configuration. The height and diameter of the windings remain unchanged, and only the effect of the radial distances of the windings from the core is examined.

Table 3. Geometrical parameters of winding order a.

Windings Parameter	Inner Radius [mm]	Outer Radius [mm]	Height [mm]
LV Winding	320	388	966
HV Winding	412	486.5	914
Tap Winding	511.5	522	630

Table 4. Geometrical parameters of winding order b.

Windings Parameter	Inner Radius [mm]	Outer Radius [mm]	Height [mm]
LV Winding	320	388	966
Tap Winding	412	422.5	630
HV Winding	447.5	522	914

Table 5. Geometrical parameters of winding order c.

Windings Parameter	Inner Radius [mm]	Outer Radius [mm]	Height [mm]
Tap Winding	320	330.5	630
LV Winding	355.5	423.5	966
HV Winding	448.5	522	914

Table 6. Ampere-turn values of the linear and reverse OLTC

$\theta_{Reference} = \theta_{LV}$ Tap Position	$\theta_1 = \theta_{LV}$	$\theta_{2,linear} = \theta_{HV} - \theta_{LV}$	$\theta_{2,reverse} = \theta_{HV} - \theta_{LV}$
19-step	1.00	0.02	0.02
18-step		0.038	0.038
17-step		0.056	0.056
16-step		0.074	0.074
15-step		0.09	0.09
14-step		0.106	0.106
13-step		0.122	0.122
12-step		0.137	0.137
11-step		0.151	0.151
10-step		0.165	0
9-step		0.178	-0.02
8-step		0.191	-0.038
7-step		0.204	-0.056
6-step		0.216	-0.074
5-step		0.228	-0.09
4-step		0.239	-0.106
3-step		0.251	-0.122
2-step		0.261	-0.137
1-step		0.272	-0.151

5 Results

To investigate the impact of the tap changer type on the short-circuit impedance, a transformer with the electrical and geometric specifications listed in Table 2 has been studied. Given the differing structures of each tap changer, which result in variations in the transformer's electrical parameters, the short-circuit inductance corresponding to each type at each voltage adjustment step are presented in Table 8 and Table 9.

About Table 8, it can be observed that the short-circuit inductance values differ across various tap changer designs. Based on the average values, the coarse-fine design exhibits the highest inductance, while the reverse design shows the lowest. Regarding the variations in the short-circuit inductance across different taps within each design, as well as considering the current distribution characteristics illustrated in Figures 7 to 9, it is evident that the nominal tap position in both the coarse-fine and linear designs is centrally located. Conversely, in the reverse design, this nominal tap is positioned at the lower tap. In other words, in the coarse-fine and linear designs, the nominal tap significantly influences the short-circuit inductance, whereas, in the reverse design, the nominal tap does not have a notable impact on the short-circuit inductance value. Consequently, based on the data presented in Table 8 and Fig. 8, it can be concluded that the short-circuit inductance in the reverse design is consistently lower across all taps compared to the other two designs. Considering Eq. 11, Table 9 presents the percentage impedance values for three types of tap changers across all taps. According to standard regulations, an allowable error of 10 percent in percentage short-circuit impedance is established. From the data in the table and corresponding Fig. 10, it is evident that the analytical results fall within this acceptable range, with only one instance of deviation occurring at the upper tap of the coarse-fine design. Given the assumptions of the previously mentioned analytical method, this level of error is both predictable and acceptable. Therefore, considering the significance of percentage short-circuit impedance in transformer design and the variable short-circuit inductance across different tap changer designs, a thorough examination and careful selection of an appropriate tap changer design are very important.

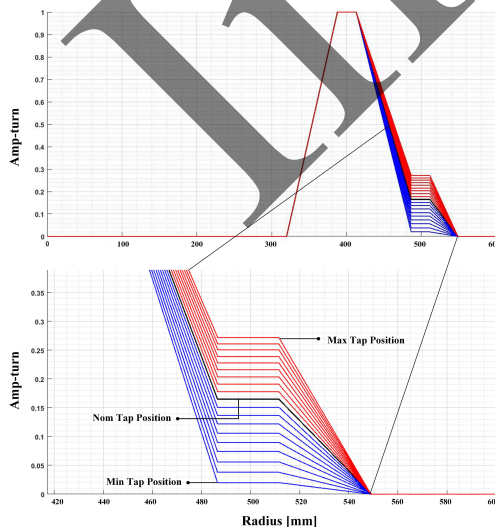
In the following, we will examine the arrangement and positioning of the windings in relation to each other and its effect on the inductance of the transformer. According to Eq. 1 and Figures 12 to 14, it can be observed that the ampere-turn distribution varies among the three winding orders, defined as (a) LV-HV-Tap windings, (b) LV-Tap-HV windings, and (c) Tap-HV-LV windings. In all cases, the tap changer winding is electrically connected to the HV winding, and the total ampere-turns of the windings equals zero. Considering that the calculations assume impedance transfer to the primary side of the transformer, and that the relationships are normalized on the low-voltage side, the ampere-turns of the LV winding always equal 1. With changes in the positioning of the tap changer winding, the distribution of ampere-turns in both the HV and tap windings (which carry the same current) is altered. These changes lead to variations in the magnetic energy of the transformer and consequently its inductance. As shown in Table 10, these changes in inductance values can be observed. A closer examination of the Table reveals that the changes in case (a) and (b)

Table 7. Ampere-turn values of the coarse-fine OLTC

$\theta_{Reference} = \theta_{LV}$ Tap Position	$\theta_1 = \theta_{LV}$	$\theta_2 = \theta_{HV} - \theta_{LV}$	$\theta_3 = \theta_2 - \theta_{Coarse}$
19-step		0.02	-
18-step		0.038	-
17-step		0.056	-
16-step		0.074	-
15-step		0.09	-
14-step		0.106	-
13-step		0.122	-
12-step		0.137	-
11-step		0.151	-
10-step	1.00	0.165	-
9-step		0.179	0.017
8-step		0.192	0.033
7-step		0.205	0.049
6-step		0.217	0.063
5-step		0.229	0.077
4-step		0.24	0.091
3-step		0.252	0.105
2-step		0.262	0.117
1-step		0.273	0.13

Table 8. Short-circuit inductance values

Tap Position	Tapping Range [%]	L_{Linear} [H]	L_{Coarse} [H]	$L_{Reverse}$ [H]
19(Lowest)	0.85	0.0129	0.0128	0.0124
18	0.87	0.0131	0.0129	0.0124
17	0.88	0.0132	0.0131	0.0125
16	0.90	0.0133	0.0132	0.0125
15	0.92	0.0134	0.0134	0.0125
14	0.93	0.0136	0.0135	0.0125
13	0.95	0.0137	0.0137	0.0125
12	0.97	0.0138	0.0139	0.0125
11	0.98	0.0139	0.0141	0.0125
10(Nom)	1.00	0.0141	0.0140	0.0125
9	1.02	0.0142	0.0141	0.0127
8	1.03	0.0143	0.0143	0.0129
7	1.05	0.0144	0.0144	0.0131
6	1.07	0.0145	0.0146	0.0133
5	1.08	0.0146	0.0148	0.0134
4	1.10	0.0147	0.0149	0.0135
3	1.12	0.0147	0.0151	0.0137
2	1.13	0.0148	0.0152	0.0138
1(Highest)	1.15	0.0149	0.0154	0.0138
Average	-	0.0140	0.0132	0.0128

**Fig.7** Ampere-turn distribution of linear OLTC**Table 9.** Short-circuit impedance values

Tap Position	Tapping Range [%]	$U_{klinear}$ [%]	$U_{kcoarse-fine}$ [%]	$U_{kreverse}$ [%]
19(Lowest)	0.85	10.12	10.04	9.7
18	0.87	10.28	10.12	9.7
17	0.88	10.36	10.28	9.81
16	0.90	10.44	10.36	9.81
15	0.92	10.51	10.51	9.81
14	0.93	10.67	10.59	9.81
13	0.95	10.75	10.75	9.81
12	0.97	10.83	10.91	9.81
11	0.98	10.91	11.06	9.81
10(Nom)	1.00	11.06	10.99	9.81
9	1.02	11.14	11.06	9.99
8	1.03	11.22	11.22	10.12
7	1.05	11.30	11.30	10.28
6	1.07	11.38	11.46	10.44
5	1.08	11.46	11.61	10.51
4	1.10	11.53	11.69	10.59
3	1.12	11.53	11.85	10.75
2	1.13	11.61	11.93	10.83
1(Highest)	1.15	11.69	12.08	10.83
Average	-	10.98	11.04	10.11

are ascending, while those in cases (b) are descending. Therefore, the variations in impedance with changes in load and tap position differ among these three scenarios.

6 CONCLUSION

As the demand for reliable and efficient power delivery systems intensifies with the expansion of power networks, the role of tap changers in voltage regulation becomes increasingly vital. This paper provided a comprehensive overview of the different types of on-load tap changers (OLTCs) and their configurations—linear, reverse, and coarse-fine—highlighting their respective functionalities in maintaining voltage stability under varying load conditions. The impact of tap changer design on short-circuit impedance was underscored, emphasizing the importance of understanding how variations in leakage inductance across different tap settings could affect transformer performance and reliability. In this article, the importance of the tap changer type and the positioning of the tap winding within the active part structure of the transformer is discussed. Understanding the relationship between winding order and impedance swings is essential for designing transformers that can handle varying electrical demands without compromising efficiency or stability. The analytical approach employed in this study offers valuable insights into the inductive characteristics of transformers under various operational scenarios, providing a foundation for further exploration of numerical methods that may yield even more precise results. Ultimately, this research contributed to the ongoing discourse on optimizing transformer design and operational efficiency, thereby supported the comprehensive goal of enhancing voltage regulation in modern power systems.

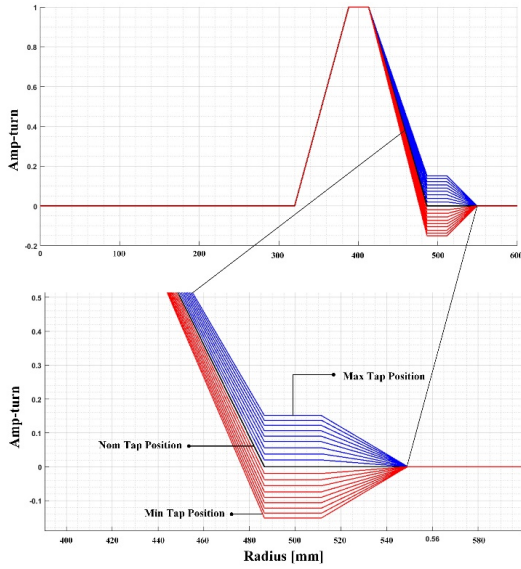


Fig.8 Ampere-turn distribution of reverse OLTC

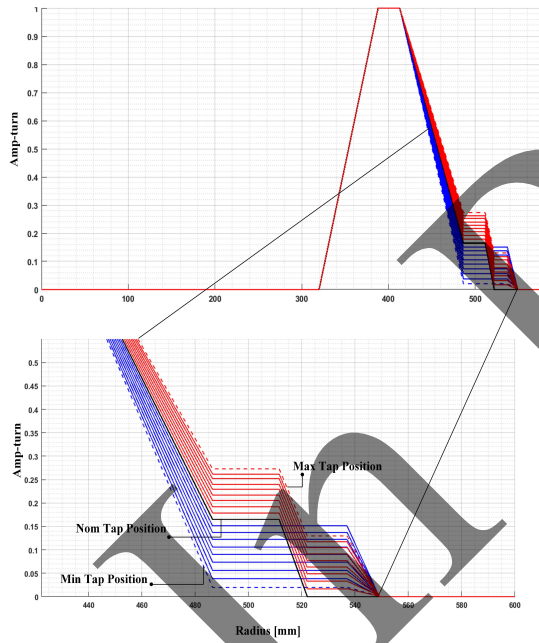


Fig.9 Ampere-turn distribution of coarse-fine OLTC

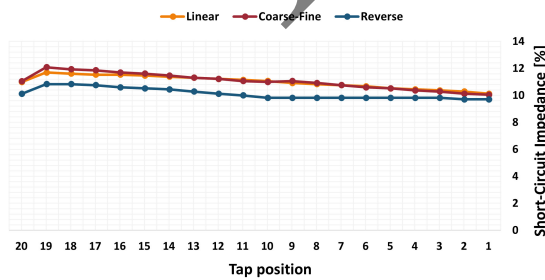


Fig. 11 Short-circuit impedance of different tap positions

Table 10. Short-circuit impedance values of winding order

Tap Position	Tapping Range [%]	L_a [H]	L_b [H]	L_c [H]
19(Lowest)	0.85	0.0127	0.0192	0.0139
18	0.87	0.0129	0.0190	0.0141
17	0.88	0.0130	0.0188	0.0142
16	0.90	0.0132	0.0184	0.0144
15	0.92	0.0133	0.0081	0.0145
14	0.93	0.0135	0.0179	0.0143
13	0.95	0.0136	0.0170	0.0142
12	0.97	0.0137	0.0173	0.0139
11	0.98	0.0143	0.0176	0.0154
10(Nom)	1.00	0.0136	0.0163	0.0145
9	1.02	0.0138	0.0162	0.0148
8	1.03	0.0140	0.0161	0.0150
7	1.05	0.0143	0.0159	0.0151
6	1.07	0.0144	0.0158	0.0153
5	1.08	0.0146	0.0156	0.0154
4	1.10	0.0147	0.0155	0.0156
3	1.12	0.0149	0.0153	0.0157
2	1.13	0.0150	0.0151	0.0157
1(Highest)	1.15	0.0151	0.0149	0.0158

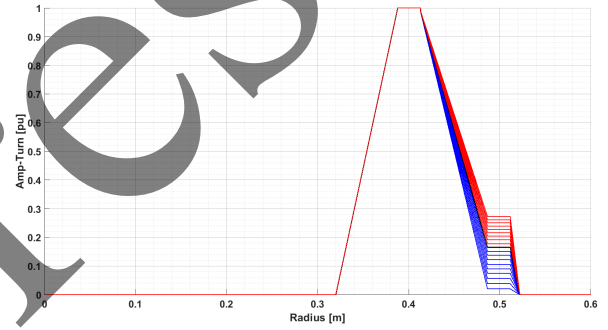


Fig. 12 Ampere-turn distribution of winding order a

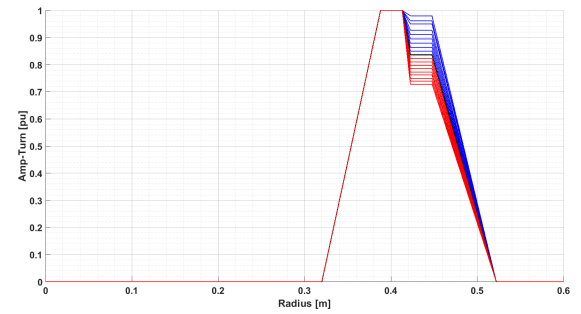


Fig. 13 Ampere-turn distribution of winding order b

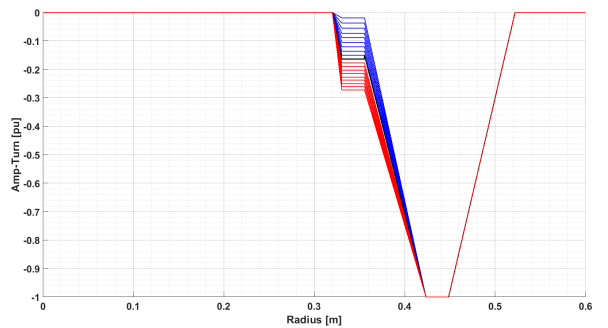
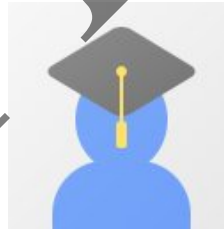


Fig. 14 Short-circuit impedance of different tap positions

References

- [1] Ferreira, Carlos Aparecido and Prada, Ricardo Bernardol, "Improved model for tap-changing transformer," IET Generation, Transmission & Distribution, Vol.7, pp.1289-1295, 2013.
- [2] Hatzargyriou, Nikos and Milanovic, Jovica and Rahmann, Claudia and Ajjarapu, Venkataramana and Canizares, Claudio and Erlich, Istvan and Hill, David and Hiskens, Ian and Kamwa, Innocent and Pal, Bikash and others, "Definition and classification of power system stability revisited & extended," IEEE Transactions on Power Systems, Vol.36, pp.3271–3281, 2020.
- [3] Tshivhase, Ndamulelo and Hasan, Ali N and Shongwe, Thokozani, "A fault level-based system to control voltage and enhance power factor through an on-load tap changer and distributed generators," IEEE Access, Vol.9, pp.34023–34039, 2021.
- [4] Base, MK, "On-load tap-changers for power transformers," Regensburg, Germany, 2013.
- [5] Kramer, Axel, "On-load Tap-changers for Power Transformers: Operation, Principles, Applications and Selection," Maschinenfabrik Reinhausen, 2014.
- [6] Zhang, Chenchen and Ge, Wenqi and Xie, Yi and Li, Yingying "Comprehensive analysis of winding electromagnetic force and deformation during no-load closing and short-circuiting of power transformers", IEEE Access, Vol.9, pp. 73335–73345, 2021.
- [7] Taghilou, Mahsa and Mirsalim, Mojtaba, "Impact of Tap Changer Configurations on Short-Circuit Inductance of a Transformer: An Analytical Approach," IEEE, 2024 4th International Conference on Electrical Machines and Drives (ICEMD), IEEE, 2024.
- [8] "Power transformers - Part 1: General," IEC 60076-1:2011.
- [9] "IEEE Standard for General Requirements for Liquid-Immersed Distribution, Power, and Regulating Transformers" IEEE C57.12.00-2015.
- [10] Taghilou, Mahsa and Mirsalim, Mojtaba and Eslamian, Morteza and Teymouri, Ashkan, "Analyzing the Impact of Cover Design on Stray Losses in High Current Distribution Transformers Based on 3D-FEM Analysis," IEEE, 2024 28th International Electrical Power Distribution Conference (EPDC), pp.1–9, 2024.
- [11] Alves, Bruno S and Kuo-Peng, Patrick and Dular, Patrick, "Contribution to power transformers leakage reactance calculation using analytical approach," International Journal of Electrical Power & Energy Systems, Elsevier, Vol.105, pp.470–477, 2019.
- [12] Fouineau, Alexis and Raulet, Marie-Ange and Lefebvre, Bruno and Bu-rais, Noé'l and Sixdenier, Fabien, "Semi-analytical methods for calculation of leakage inductance and frequency-dependent resistance of windings in transformers," IEEE Transactions on magnetics, Vol.54, pp.1–10, 2018.
- [13] Cardoso, Antonio J Marques and others, "Leakage inductances calculation for power transformers interturn fault studies," Results in Engineering, Elsevier, Vol.30, pp.1213–1220, 2014.
- [14] Del Vecchio, Robert and Del Vecchio, Robert M and Poulin, Bertrand and Feghali, Pierre and Shah, Dilipkumar and Ahuja, Rajendra, Fred 'eric, "Transformer design principles," CRC press, 2017.
- [15] Amoiralis, Eleftherios I and Tsili, Marina A and Kladas, Antonios, "Transformer design and optimization: a literature survey," IEEE Transactions on power delivery, Vol.24, pp.1999–2024, 2009.
- [16] Dawood, Kamran and Cinar, Mehmet Aytac and Alboyaci, Bora and Sonmez, Olus, "Calculation of the leakage reactance in distribution transformers via numerical and analytical methods," Journal of Electrical Systems, Vol.15, pp.213–221, 2019.
- [17] de Metz-Noblat, B and Dumas, F and Poulain, C, "Cahier technique no. 158," 2005.

Biographies



Mahsa Taghilou (Student Member, IEEE) is currently pursuing a PhD in Electrical Engineering at Amirkabir University of Technology, where she is a member of the Electrical Machines and Transformers Research Laboratory (EMTRL).

Her research focuses on the electromagnetic behavior of power transformers, aiming to enhance their design and operational efficiency through innovative optimization techniques.



Mojtaba Mirsalim (IEEE Life Senior Member) received a B.S. degree in double major electrical/nuclear engineering and an M.S. degree in nuclear engineering from the University of California at Berkeley, Berkeley, CA, USA, in 1978 and 1980, respectively, and the Ph.D. degree in electrical engineering from

Oregon State University, Corvallis, OR, USA, in 1986. Since 1987, he has been with the Amirkabir University of Technology, Tehran, Iran, where he has served five years as the Vice-Chairperson and more than seven years as the

General Director in Charge of Academic Assessments and is currently a Full Professor with the Department of Electrical Engineering, where he teaches courses and conducts research in energy conversion, electrical machine design, and hybrid vehicles, wireless power transfer, among others. He is the Founder and Director of the Electrical Machines and Transformers Research Laboratory (EMTRL). Mirsalim has coauthored over 270 international journal articles and conference papers, four books on electric machinery and finite element method (FEM), and holds 23 patents, two of which are U.S. patents. His special fields of interest include the design, analysis, and optimization of electric machines, renewable energy, hybrid vehicles, and FEM. He is also an editor for the IEEE Transactions on Energy Conversion, and the Iranian Journal of Science and Technology, Transactions of Electrical Engineering.

in Press